J Neuropathol Exp Neurol
Vol. 77, No. 11, November 2018, pp. 1039–1054
doi: 10.1093/jnen/nly085

ORIGINAL ARTICLE

A Revised Diagnostic Classification of Canine Glioma: Towards Validation of the Canine Glioma Patient as a Naturally Occurring Preclinical Model for Human Glioma

Jennifer W. Koehler, DVM, PhD, Andrew D. Miller, DVM, C. Ryan Miller, MD, PhD, Brian Porter, DVM, Kenneth Aldape, MD, Jessica Beck, DVM, Daniel Brat, MD, PhD, Ingrid Cornax, DVM, PhD, Kara Corps, DVM, Chad Frank, DVM, MS, Caterina Giannini, MD, PhD, Craig Horbinski, MD, PhD, Jason T. Huse, MD, PhD, M. Gerard O'Sullivan, MVB, MSc, PhD, Daniel R. Rissi, DVM, MS, PhD, R. Mark Simpson, DVM, PhD, Kevin Woolard, DVM, PhD, Joanna H. Shih, PhD, Christina Mazcko, BS, Mark R. Gilbert, MD, and Amy K. LeBlanc, DVM

Abstract

The National Cancer Institute-led multidisciplinary Comparative Brain Tumor Consortium (CBTC) convened a glioma pathology board, comprising both veterinarian and physician neuropathologists, and conducted a comprehensive review of 193 cases of canine glioma. The immediate goal was to improve existing glioma classification methods through creation of a histologic atlas of features, thus yielding greater harmonization of phenotypic characterization. The long-term goal was to support future incorporation of clinical outcomes and genomic data into proposed simplified diagnostic schema, so as to further bridge the worlds of veterinary and physician neuropathology and strengthen validity of the dog as a naturally occurring, translationally relevant animal model of human glioma. All cases were morphologically reclassified according to a new schema devised by the entire board, yielding a majority opinion diagnosis of astrocytoma (43, 22.3%), 19 of which were low-grade and 24 high-grade, and oligodendroglioma (134, 69.4%), 35 of which

From the Department of Pathobiology, College of Veterinary Medicine, Auburn University, Auburn, Alabama (JWK); Department of Biomedical Sciences, Section of Anatomic Pathology, College of Veterinary Medicine, Cornell University, Ithaca, New York (ADM); Department of Pathology and Laboratory Medicine (CRM); Department of Neurology (CRM); and Department of Pharmacology (CRM), Lineberger Comprehensive Cancer Center and Neuroscience Center, University of North Carolina School of Medicine, Chapel Hill, North Carolina; Department of Veterinary Pathobiology, College of Veterinary Medicine and Biomedical Sciences, Texas A&M University, College Station, Texas (BP); Laboratory of Pathology, Center for Cancer Research, National Cancer Institute, National Institutes of Health, Bethesda, Maryland (KA); Laboratory of Human Carcinogenesis, Center for Cancer Research, National Cancer Institute, National Institutes of Health, Bethesda, Maryland (JB); Department of Pathology, Feinberg School of Medicine, Northwestern University, Chicago, Illinois (DB); Department of Pediatrics, University of California-San Diego, San Diego California (IC); National Institute of Neurological Disorders and Stroke, National Institutes of Health, Viral Immunology and Intravital Imaging Section, Bethesda, Maryland (KC); Department of Microbiology, Immunology, and Pathology, College of Veterinary Medicine and Biomedical Sciences, Colorado State University, Ft. Collins, Colorado (CF); Division of Anatomic Pathology, Department of Laboratory Medicine and Pathology, Mayo Clinic College of Medicine, Rochester, Minnesota (CG); Department of Pathology (CH); and Department of Neurosurgery (CH), Feinberg School of Medicine, Northwestern University, Chicago, Illinois; Departments of Pathology and Translational Molecular Pathology, The University of Texas MD Anderson Cancer Center, Houston, Texas (JTH); Masonic Cancer Center Comparative Pathology Shared Resource and Department of Veterinary Population Medicine, College of Veterinary Medicine, University of Minnesota, St. Paul, Minnesota (MGO'S); Department of Pathology and Athens Veterinary Diagnostic Laboratory, College of Veterinary Medicine, University of Georgia, Athens, Georgia (DRR); Center for Cancer Research, National Cancer Institute, National Institutes of Health, Molecular Pathology Unit, Laboratory of Cancer Biology and Genetics, Bethesda, Maryland (RMS); Department of Pathology, Microbiology, and Immunology, School of Veterinary Medicine, University of California-Davis, Davis, California (KW); Biometrics Research Program, Division of Cancer Treatment and Diagnosis, National Cancer Institute, National Institutes of Health, Bethesda, Maryland (JS); Comparative Oncology Program, Center for Cancer Research, National Cancer Institute, National Institutes of Health, Bethesda, Maryland (CM); National Institute of Neurological Disorders and Stroke and the Center for Cancer Research, National Cancer Institute, National Institutes of Health, NeuroOncology Branch, Bethesda, Maryland (MRG); and National Cancer Institute, National Institutes of Health, Comparative Oncology Program, Center for Cancer Research, Bethesda, Maryland (AKL)

Send correspondence to: Amy K. LeBlanc, DVM, Center for Cancer Research, Comparative Oncology Program, 37 Convent Dr, Room 2144, National Cancer Institute, National Institutes of Health, Bethesda, MD 20892; E-mail: amy.leblanc@nih.gov

Jennifer W. Koehler, Andrew D. Miller, C. Ryan Miller, and Brian Porter have contributed equally to this work.

This research was supported in part by the Intramural Research Program of the National Institutes of Health (NIH), NCI, Center for Cancer Research. Jessica Beck and Kara Corps are supported in part by the NIH Comparative Biomedical Scientist Training Program, in partnership with Purdue University (Jessica Beck) and North Carolina State University (Kara Corps). The results and interpretations do not reflect the views of the US Government.

The authors have no duality or conflicts of interest to declare.

Supplementary Data can be found at academic.oup.com/jnen.

were low-grade and 99 were high-grade. Sixteen cases (8.3%) could not be classified as oligodendroglioma or astrocytoma based on morphology alone and were designated as undefined gliomas. The simplified classification scheme proposed herein provides a tractable means for future addition of molecular data, and also serves to highlight histologic similarities and differences between human and canine glioma.

Key Words: Canine, Comparative, Glioma.

INTRODUCTION

Comparative oncology is a growing field of study centered around exploration of naturally occurring cancers in nonhuman species, such as pet dogs, as a parallel and complementary model for human cancer research efforts (1–5). In 2015, the National Cancer Institute's intramural Comparative Oncology Program created the Comparative Brain Tumor Consortium (CBTC). The mission of this multidisciplinary consortium is to discover and develop new treatments and diagnostic strategies for brain tumors through full integration of the canine brain tumor patient into all aspects of brain tumor research. Utilizing a working group organizational structure, the CBTC membership identified several key initiatives designed to address gaps in knowledge that may represent barriers to achieving this mission (6). Specific projects were designed by the members to fill these critical knowledge gaps, while also galvanizing the field around the concept that canine central nervous system (CNS) malignancies could provide unique opportunities to advance drug discovery and development for benefit of both species.

Canine patients represent a relatively diverse population in which many diseases of interest occur spontaneously. There are recent examples of successful efforts to compare canine and human neoplasms and assess the suitability of dogs as preclinical models (7–11). While it is widely acknowledged that no single animal model can accurately recapitulate human disease, many models, including neurosphere cultures, patient-derived xenografts, and genetically engineered mice are informative in specific instances (12–14). The clear advantages afforded by the pet dog that spontaneously develops glioma include natural coevolution of tumor and surrounding microenvironment, intratumoral heterogeneity, a relevant blood-brain barrier, and an intact immune system (15–19). In that sense, the dog may be considered a robust intermediate animal model for human glioma, should appropriate and relevant histologic and molecular features be defined.

It is critically important to determine how brain neoplasms that arise naturally in dogs relate to human tumors with respect to histologic, molecular, and genetic signatures. While some investigations into the molecular landscape of canine gliomas have been conducted, and do suggest some potential similarities and differences to human glioma, these reports are limited by size and scope, and are somewhat hindered by availability of canine-specific reagents and tools (20–28). Both veterinarian and physician members of the CBTC agreed that a systematic assessment of canine gliomas as a comparative model of human gliomas must begin with a critical eye to the initial comprehensive descriptive diagnosis. In human medicine, the combination of histopathology and molecular genetic data drastically changed the diagnostic approach to gliomas and prompted a reexamination of prognostic paradigms in relation to gross and histologic appearance. From high-density genomic datasets, select key molecular markers (IDH, MGMT, 1p19q, ATRX) have been identified and incorporated into routine tumor assessment as diagnostic, prognostic, and/or predictive biomarkers. This layering of histopathology with molecular genetic pathology has begun to result in more accurate classification and better prognostic indicators for human patients (29, 30).

Veterinary anatomic pathologists have relied on the World Health Organization (WHO) Tumor Fascicle Histological Classification of Tumors of the Nervous System of Domestic Animals for diagnostic guidance since its publication in 1999, with the addition of immunohistochemical markers of glial populations that have become more readily available in the intervening years (31). In human neuropathology, the introduction of the 2016 WHO Classification of Tumors of the Central Nervous System (2016 WHO) represented a departure from traditional principles of diagnosis by incorporating molecular features into the classification scheme (32). Prior to this update, neuropathologists used the schema provided by the 2007 WHO, which grouped tumors based on morphologic characteristics predictive of clinical outcomes, but allowed for molecular features to be included as diagnostic, prognostic, and/or predictive data within diagnoses established by conventional histopathology (33). As advances in molecular diagnostics become increasingly established within both the human and veterinary oncology communities, we felt it was important that our efforts lay an appropriate groundwork where molecularly derived phenotypic data could be added into a morphologic diagnosis, thus further linking the classification of glioma subtypes between dogs and humans. In anticipation of an imminent expansion of genetic information in canine glioma, the group sought to design a simplified, decision tree-based algorithm for use in the diagnosis of canine gliomas with the comparative input of physician neuropathologists. The ultimate goal is to, as has been accomplished in humans, identify from high-density molecular profiling, a panel of key biomarkers that eventually can be incorporated alongside the histologic classification method proposed herein. This project was designed as the first step toward achieving that goal.

To that end, the CBTC pathology and molecular markers working group prioritized a comparative study of naturally occurring canine gliomas, for which the following immediate goals were identified: 1) to describe the relevant clinical and pathologic features, underscoring similarities and differences between dog and human glioma, through creation of a histologic atlas which highlights the relevant canine subtypes and the existing supporting data that justifies further definition and development of the companion dog as a preclinical/translational model; and 2) to create a new classification scheme to promote diagnostic consistency across veterinary institutions and to harmonize future comparative research and hypothesis-based investigations designed to aid in clinical management of canine glioma patients. We also examined the utility and reliability of immunohistochemical

markers in a subset of canine gliomas. We anticipate that this will allow integration of reproducible, descriptive diagnoses with forthcoming genetic information, enabling our consortium to compare dog and human gliomas at multiple levels. This project serves not only to produce a classification scheme that can be adopted to provide more consistent diagnoses, but also serves to further endorse the field of comparative neuropathology and advance the concept of comparative cancer research.

MATERIALS AND METHODS

Creation of the Comparative Glioma Pathology Board

To execute the stated goals, a 15-member board comprising both physician neuropathologists (6) and veterinary pathologists (9) with expertise in canine neuropathology was created. All members agreed to participate in a series of meetings, both virtual and in-person, designed to educate the members on the landscape of both human and canine glioma diagnostic methodology.

Tissue Procurement

The timeline of events in this initiative are outlined in Figure 1. A call for archived canine glioma tissues in paraffin blocks was sent out to CBTC veterinary member institutions to populate a case set for review. A diagnosis of glioma, based upon review of histopathology reports provided by the submitting institution, agnostic of subtype, was required. Case material harvested from surgical biopsy conducted as a part of routine veterinary care or at postmortem necropsy was allowed as long as sufficient tissue was present to support a panel of immunohistochemical markers, described below, in addition to a centralized review of a representative hematoxylin and eosin (H&E)-stained section. Patient demographic data and clinical outcome data were collected from these cases. Eleven academic institutions (Auburn University, Colorado State University, Cornell University, University of Georgia, University of Minnesota, Ohio State University, University of Pennsylvania, Purdue University, University of Tennessee, Texas A&M University, and Virginia Tech) initially submitted a total of 262 cases, from which a set of 147 cases were selected for further review, based upon quantity of tissue in the paraffin block, overall sample quality, and financial considerations of the scope of the project. These 147 cases were confirmed to have adequate quantity and quality of tumor tissue by review of the scanned H&E images, conducted at 40× magnification utilizing a Leica Aperio ScanScope CS (Leica Biosystems, Buffalo Grove, IL).

Immunohistochemical Methods

After review of freshly stained H&E sections to assure adequate diagnostic quality of the samples, additional 5-μm-thick formalin-fixed, paraffin-embedded sections were used for immunohistochemistry (IHC) performed at Cornell. Sections were deparaffinized in xylene and hydrated in graded ethanol. Endogenous peroxidase activity was blocked with 3% peroxide for all antibodies. Antibodies for immunolabeling were as follows: Ki67 (catalog number: M7240; Dako, Carpinteria, CA; 60-minute incubation at a dilution of 1: 50), CNPase (catalog number: AB6319; Abcam, Cambridge, MA; 15-minute incubation at a dilution of 1: 2000), Olig2 (catalog number: AB109186; Abcam; 60-minute incubation at a dilution of 1: 2000), neurofilament (catalog number: M0762; Dako; 15-minute incubation at a dilution of 1: 300), and GFAP (catalog number: Z0334; Dako; 60-minute incubation at a dilution of 1: 5000). All stains were performed using the Leica BOND Max Automated IHC staining system. Sections were dewaxed with Bond Dewax Solution (Leica; catalog number: AR9222) followed by heat epitope retrieval with bond epitope retrieval solution 1 for 30 minutes (Leica; catalog number: AR9961). Sections then had a peroxide block applied (Leica; catalog number DS9800). Depending on the marker, PV-AP-Anti-Mouse IgG reagent was applied for 30 minutes (Ki67) or 10 minutes (CNPase, neurofilament) (Leica; catalog number DS9390). For Olig2 and GFAP, polymer was applied for 10 minutes following the primary antibody (Leica; catalog number DS9800). For all antibodies, Leica Bond Polymer Refine detection was applied for 10 minutes (Leica; catalog number DS9800), followed by hematoxylin for 5 minutes. Positive control tissues included canine lymph node (Ki67) and brain (CNPase, Olig2, neurofilament, GFAP), and isotype-matched antibodies were used as negative controls in adjacent tissue sections. For CNPase, GFAP, and Olig2, slides were scored on a scale of 0–3 as follows: 0 = no labeling, 1 = <25% labeling, 2 = 25–75% labeling, and 3 = >75% labeling. For Ki67, an approximation of percent positive cells was recorded. Lastly, for neurofilament, the extent of tumor infiltration into the adjacent parenchyma was subjectively determined.

Training Phase

In order to familiarize physician neuropathologists with the histologic landscape of canine glioma, a training webinar was held. Representative canine gliomas (n = 10) were shown to highlight classic features such as astrocytic and oligodendroglial cellular morphology, patterns of necrosis, infiltration, and microvascular proliferation. The webinar lead (J.W.K.) assembled photomicrographs of H&E and IHC slides, along with original diagnosis, key diagnostic features, and diagnostic features that created a dilemma, into a slide deck that was reviewed and discussed by all pathologists. The cases provided for this review were nonrandomly selected to demonstrate a wide range of diagnostic features present in canine gliomas, as well as a variety of artifacts that occur as a result of postmortem degeneration, poor fixation, and excess time in formalin prior to IHC. The perceived overrepresentation of oligodendrogliomas in dogs was discussed, as was the compact nature of some canine oligodendrogliomas despite high-grade features and anaplastic cellular morphology. It was also emphasized that dogs develop nonglioma CNS tumors, such as histiocytic sarcoma, that can be poorly differentiated and require IHC to assist in determination of cellular composition. Selected deidentified human case material was also reviewed (led by C.R.M.) to demonstrate common human glioma

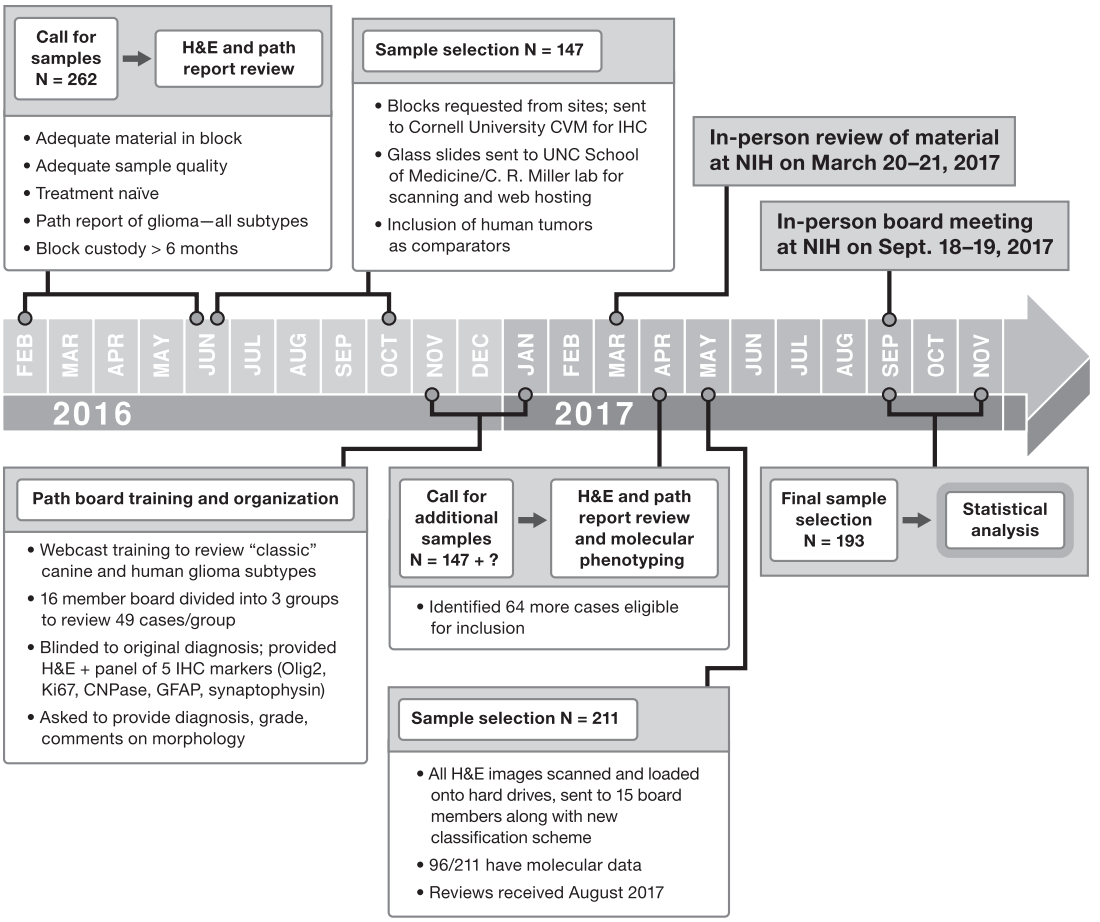

FIGURE 1. Timeline of events and workflow for the Comparative Brain Tumor Consortium glioma pathology board.

features to the veterinary neuropathologists. The inclusion of molecular genetic data was emphasized for diagnosis of human glioma.

After review and verification of sample quality by H&E staining, sets of approximately 50 cases were distributed among the pathology board members, whom were divided into 3 teams of 4 or 5 members comprising both veterinarian and physician neuropathologists. Slides were optically scanned in the UNC Translational Pathology Laboratory using a Leica Aperio ScanScope XT (Leica Biosystems) equipped with a 20× objective. SVS files were hosted for review by all board members on a customized instance of Leica eSlide Manager. Pathologists were asked to review cases based on discussion points covered in the webinar training; physicians were asked to provide insight on how the canine tumors would be diagnosed under human histologic review criteria, as per the 2007 WHO guidelines (30).

An in-person review of this case material was conducted on the NIH campus, with the goal of gauging concordance and discordance amongst pathologists of both scientific disciplines as to the diagnosis of a variety of canine glioma subtypes. During this meeting, the board reviewed selected highly concordant and discordant cases, including the IHC findings, and discussed the commonalities and differences between canine and human glioma. The board collectively felt that the absence of widespread access to molecular phenotyping for canine tumors, coupled with the inherent issues of IHC, such as limited availability of validated canine-specific antibodies and inconsistent methods of tissue fixation, make direct comparisons with human glioma subtypes based on histopathology challenging.

From this analysis, the board produced a consensus set of criteria to evaluate, diagnose, and grade tumors that could be uniformly applied (Table 1). Current human glioma classification is heavily weighted towards molecular genetic characterization, improvement that was achieved through molecular characterization guided by the tumor morphology. The revised and simplified classification scheme, including a feature-based algorithm (Fig. 2), is constructed to support the addition of molecular phenotypic profiles, thus aiding harmonization of canine glioma classification and permitting better comparisons to human gliomas. In support of this algorithm, we also conducted a statistical analysis of reviewer performance across specific histologic features, described below.

Classification Phase

A subsequent round of reviews, wherein the entire board reviewed all case material, was conducted. In this same interval, a comprehensive parallel molecular analysis project came

TABLE 1. Histologic Descriptors and Definitions Collectively Defined and Applied by CBTC Glioma Pathology Board Members to Arrive at a Histologic Classification and Grade Assignment for 193 Canine Tumors

Histologic Classification	Descriptors
Oligodendroglioma; so designated if >80% of tumor meets these criteria	• Mostly round nuclei; coarse chromatin pattern; scant to moderate eosinophilic or lost cytoplasm (artifact); pseudo-rosettes; secondary structures; nuclear rowing; myxoid/mucinous matrix ± lakes; branching capillaries; mineralization; nuclear molding • Fixation artifacts with flattened and condensed nuclei can be present
Astrocytoma; so designated if > 80% of tumor meets these criteria	• Oval to elongate nuclei (angular); open-faced chromatin pattern; pleomorphic cells (large nucleoli, multinucleate cells); eosinophilic, abundant cytoplasm (gemistocytic), elongate cells (pilocytic); naked nuclei; random, disorganized pattern; spindle cell morphology; rare mucin microcysts (well-defined); mineralization; eosinophilic stroma (fibrillary) • Lower degree of cellular density than typical oligodendroglioma
Undefined	• Undifferentiated cellular morphology • Biphenotypic/biphasic: Both phenotypes in high proportions (>30–40% each)
Descriptive comments	

Infiltration	• Diffuse vs. focal; challenges to assess with biopsies
	• Assessed at low magnification
	  • Compact tumor or growth pattern (no infiltration) and/or rare foci of infiltration
	  • Focal infiltration: Compact with focal/multifocal regions of infiltration
	  • Diffuse infiltration

Pseudo-palisading necrosis	• Neoplastic cells lined up perpendicularly to areas of necrosis
Microvascular proliferation	• Convoluted, glomeruloid vasculature; multilayered, hypertrophied endothelial cells; arcades of vasculature; distinguish from reactive vasculature
Necrosis	• Pattern- yes or no, exclude single cell necrosis (can note if geographic or not)
Mitosis	• Any in ten 40× high power fields of view or none in ten 40× fields
Universal features of malignancy	• Cellular atypia, anisocytosis, anisokaryosis, nuclear pleomorphism

to light, triggering an additional call for canine samples, resulting in an increase in case material from 147 to 193 cases and including material from an additional veterinary academic institution (University of California at Davis). For this phase of the project, a subcommittee of 14 reviewers worked independently (9 veterinarians, 5 physicians) to evaluate 193 cases according to the simplified methods devised during the first training phase described above. Statistical assessment of this phase of the project is described below, wherein we sought to describe how physician and veterinarian neuropathologists perform on detection of features including infiltration, mitotic activity, necrosis, and microvascular proliferation in their diagnosis of canine tumors by histology and grade.

Statistical Analysis

The statistical analysis was designed to determine inter-reviewer agreement on classification of tumor type and grade, as well as each histologic feature prompted for assessment by each pathologist. We applied methods to assess overall as well as pairwise agreement, as the latter allows the ability to see if some reviewers performed differently than others. Agreement stratified by reviewer background (MD vs DVM) was also assessed. We asked if the presence of specific pathologic features affected reviewer's assignment of tumor grade, and how a reviewer's scientific background correlated with his/her diagnosis of tumor type and grade. Finally, we sought to determine if there was correlation between specific dog breeds and prevalence of tumor type, grade and specific histologic features.

Chance-corrected reviewer agreement on the diagnosis of each dichotomous pathologic feature was determined by the intraclass correlation coefficient (ICC). The ICC was obtained from variance components which were estimated by fitting a two-way random effects model with case and reviewer as the random intercepts and pathologic feature as the binary response (34, 35). For nominal pathologic features with >2 categories, the unweighted kappa statistic was used to measure reviewer agreement (36). Confidence intervals of ICC and kappa were obtained by bootstrapping on the case level with replacement. The limits of the 95% confidence intervals were taken from the 2.5th and 97.5th percentiles of 1, 000 bootstrap samples. For this analysis, an ICC $\leq$0.4 indicated fair agreement, 0.41–0.6 moderate agreement, 0.61–0.8 substantial agreement, and >0.8 near perfect agreement.

Prevalence of each pathologic feature was defined as the average reviewer-specific detection of these features. The Bootstrap procedure was used to obtain standard errors and confidence intervals. P values for the comparison of prevalence with respect to reviewers' background (DVM vs MD) and tumor grade were obtained by Z-tests.

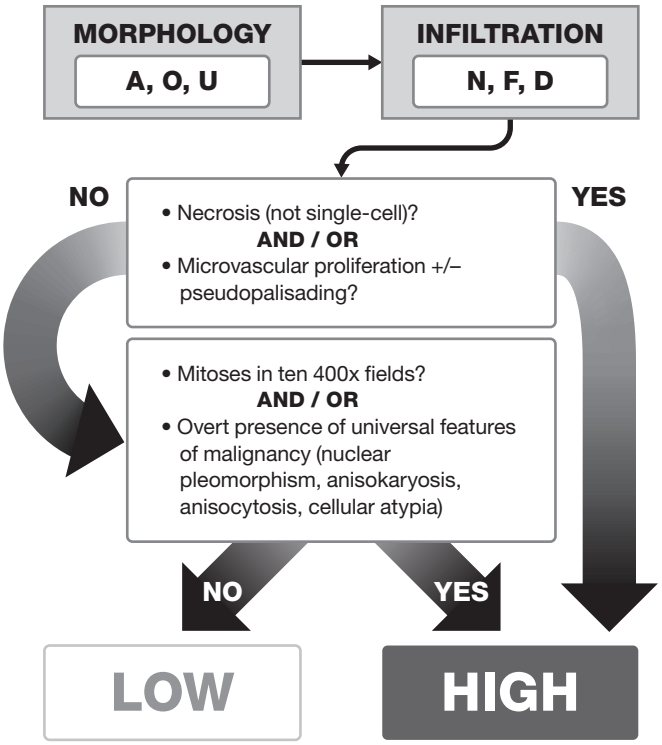

FIGURE 2. Decision-tree approach for the reclassification of 193 canine gliomas assessed by the Comparative Brain Tumor Consortium glioma pathology board. A = astrocytic morphology; O = oligodendrogial morphology; U = undefined morphology; N = no infiltration; F = focal infiltration; D = diffuse infiltration.

RESULTS

Creation of a Histologic Atlas of Canine Glioma

In order to better compare canine and human glioma, including histologic and molecular analyses, the first goal of the consortium was to develop a histologic atlas of canine glioma that would serve multiple purposes: 1) refine the diagnostic criteria of canine glioma with the benefit of comparative joint review; 2) enable future molecular classification studies; and 3) permit relevant comparisons with human glioma. Herein we provide a comprehensive assessment of 3 main subtypes of canine glioma that contain both veterinarian and physician input on diagnosis and description of the major histologic features (Table 1), and propose an updated classification system (Supplementary Data Table S1) for canine glioma diagnosis.

Table 2 captures the majority opinion diagnosis for 193 canine gliomas given by the CBTC board members, in addition to diagnoses rendered by physician members who were asked to provide a diagnosis based on an assessment of these tumors in the context of premolecular era classification methods (e.g., WHO 2007 criteria 33). Of the final set of 193 cases, the median age of dog at glioma diagnosis was 8 years (range 1–17 years). Gender distribution was as follows: 89 dogs (46%) were castrated males, 28 dogs (14.5%) were intact males, 69 dogs (36%) were spayed females, and 7 dogs (3.5%) were intact females. There were 32 cases collected via surgical biopsy and 161 cases collected at necropsy. The median age of the samples was 5 years (range <1–17 years). Multiple pure breeds were represented, as well as mixed breeds. The most common pure breed represented was the Boxer dog (n = 49 or 25%), followed by Bulldogs (American, French, English and not otherwise specified, n = 23 or 12%), Boston Terriers (n = 21 or 11%) and Pit Bulls (n = 11 or 5.7%).

Supplementary Data Table S2 captures the tumor locations and diagnoses for 188 tumors for which data was available from pathology reports and clinical data submitted by the participating veterinary institutions. Involvement of the frontal lobe, which we defined as inclusive of the olfactory lobe, as the primary site within the brain was the most frequent tumor location (66 tumors or 34%). Thirty-seven tumors (19%) had involvement of more than 1 lobe of the brain. For those tumors affecting multiple sites, lobes affected in order of frequency included frontal (n = 17 cases); temporal (n = 16 cases); parietal (n = 15 cases); thalamus/midbrain (n = 9 cases); piriform (n = 6 cases); occipital (n = 4 cases); and lateral ventricles (n = 2 cases). Two tumors affected the spinal cord. Interestingly, all tumors of primary ventricular location (n = 4) in this case set arose from and/or involved the left lateral ventricle. Six dogs had tumors that were so diffuse in nature that a primary site of involvement could not be ascertained. This is a common finding in veterinary brain tumor patients whom are often diagnosed late in the course of disease and thus present with large tumors, particularly when viewed in the context of their overall brain size.

Oligodendroglioma

As indicated in Table 1, a number of diagnostic criteria were assessed when reviewing oligodendrogliomas. The degree of invasiveness was best assessed at low magnification among tumors for which sufficient tissue was submitted to assess the tumor: normal brain interface, and was classified as diffusely infiltrative, focally infiltrative, or compact (non-infiltrative). Diffusely infiltrative tumors had uniformly ill-defined borders with invasion of adjacent gray matter, white matter, and/or leptomeninges. Infiltration at the periphery of the tumor by individual or small clusters of cells, assessed at high magnification, was common, however this did not qualify as diffusely or focally infiltrative growth in the classification criteria. Focal infiltration occurred in any region of the brain, but appeared to be more common in gray matter, with the white matter in most cases appearing to act as somewhat of a barrier to infiltration (Fig. 3A). Formation of secondary structures of Scherer, including aggregates of tumor cells surrounding neurons (perineuronal satellitosis), blood vessels (perivascular satellitosis), ependymal lining of ventricles, or clusters of cells beneath the pia matter (subpial condensation) (Fig. 3B, C), occurred along the periphery of infiltrative tumors. Compact tumors were expansile and compressed or pushed the interface with the surrounding parenchyma, but did not have evidence of infiltration at low-magnification. The degree of infiltration did not correlate with low- or high-grade features. The vast majority of oligodendrogliomas evaluated were primarily within the gray matter and either compact or focally infiltrative.

TABLE 2. Summary of the Majority Opinion* Diagnoses of 193 Canine Gliomas as Defined by the Entire Glioma Pathology Board Utilizing the Schema in Figure 2, and by Physician Neuropathology Reviewers Only Applying the 2007 WHO Guidelines for Human Glioma Diagnosis (33)

CBTC Pathology Board Majority Opinion* Diagnosis		# of Cases	% of Total	Physician Neuropathologist Majority Opinion* Diagnosis	# of Cases	% of Total
Astrocytoma	Low grade	19	9.8	Astrocytoma, Grade 2	9	4.7
	High grade	24	12.4	Astrocytoma, Grade 3	5	2.6
				Astrocytoma, Grade 4 (GBM)	24	12.4
	Total	43	22.3	Total	38	19.7
Oligodendroglioma	Low grade	35	18.1	Oligodendroglioma, Grade 2	18	9.3
	High grade	99	51.3	Oligodendroglioma, Grade 3	84	43.5
	Total	134	69.4	Total	102	52.8
Undefined glioma	Low grade	2	1	N/A	53	27.5
	High grade	14	7.3			
	Total	16	8.3	Total	53	27.5
Total		193	100.0		193	100.0

*Defined as simple majority among reviewers; CBTC panel comprised 14 reviewers (9 DVM, 5 MD); physician neuropathologist group comprised 5 reviewers.
N/A = lacked clear majority opinion among physician neuropathologists on panel; A = Astrocytoma, O = Oligodendroglioma, GBM = Glioblastoma.

With regard to cellular features, low-grade oligodendrogliomas were characterized by moderate to dense cellularity comprised of round to polygonal cells that morphologically resembled enlarged, mature oligodendrocytes (Fig. 3D). In many cases, nuclei were surrounded by a large amount of clear cytoplasm demarcated by a distinct cell membrane. This is a well-described feature colloquially referred to as a "fried-egg" or "honeycomb" appearance (31) and while it is useful in identifying oligodendrogliomas, it is worth noting that it is an artifact of autolysis and/or processing and was typically absent in biopsy and fresh necropsy samples (Fig. 3E). Low-grade tumors had a delicate network of branching thin-walled capillaries separating tumor cells into partial clusters, leading to the characteristic "chicken-wire" appearance (Fig. 3F).

In contrast, high-grade oligodendrogliomas exhibited increased anisocytosis and anisokaryosis, a high mitotic rate, and increased variation in nuclear shape, chromatin pattern, and cytoplasmic appearance. In high-grade tumors, nuclei were highly variable, with some tumors retaining round nuclei with dense chromatin and others having large, deeply cleaved, folded, or irregular nuclei with irregular chromatin patterns and sometimes quite pronounced nuclear molding (Fig. 4A). Nucleoli were distinct and numerous in some high-grade tumors. Cells varied from round to oval with minimal cytoplasm and few processes to polygonal with a large amount of clear or eosinophilic cytoplasm and numerous processes. Cells in these tumors were occasionally arranged in packet-like formations, necessitating differentiation from endocrine or neuroendocrine neoplasms. High-grade tumors had true microvascular proliferation, defined as blood vessels lined by multiple layers of hypertrophied endothelial cells ± pericytes, arranged in tortuous clusters and often forming a rim along the periphery of the tumor (Fig. 4B). In some instances, these vessels had a distinctly glomeruloid appearance. Reactive blood vessels that are dilated and tortuous but lined by a single layer of hypertrophied endothelial cells (Fig. 3F) can occur outside the setting of a high-grade tumor and should not be confused with true microvascular proliferation. Likewise, clusters of closely apposed reactive blood vessels lined by a single layer of endothelium stacked upon one another (wickerwork vascular pattern) (37) can occur in low-grade oligodendroglial tumors and also should not be confused with true microvascular proliferation. Variably sized foci of coagulative necrosis or bands of serpentine necrosis with (Fig. 4C) or without (Fig. 4D) pseudo-palisading tumor cells were also found in high-grade tumors. The assessment of necrosis, with regard to tumor grade, did not include individual cell necrosis or apoptosis.

Features that were variably present regardless of low- or high-grade included small foci of mineralization (microcalcifications). Neoplastic cells were frequently arranged in rows, mimicking the "intrafascicular queueing" of white-matter oligodendrocytes. Rarely, otherwise unremarkable oligodendrogliomas had areas in which cells were clustered around vessels with a distinct nuclear-free perivascular zone, reminiscent of ependymoma architecture (Fig. 4E). Mucinous matrix, or mucin-filled microcystic spaces, were characteristic features of these tumors (Fig. 4F). Microcystic change was a feature regardless of the grade of the neoplasm. Tumors that were considered low-grade oligodendrogliomas were typically composed of a monomorphic population of cells and had a mitotic rate <1 per $400\times$ field. The 2 most important features used by the group to differentiate low- from high-grade neoplasms were microvascular proliferation and necrosis.

Astrocytoma

As opposed to oligodendrogliomas, the degree of invasiveness in astrocytomas did correlate with grade assigned by the review committee. With the exception of rare, compact tumors often located in the caudal fossa, low-grade tumors were generally of low cellularity, but typically poorly

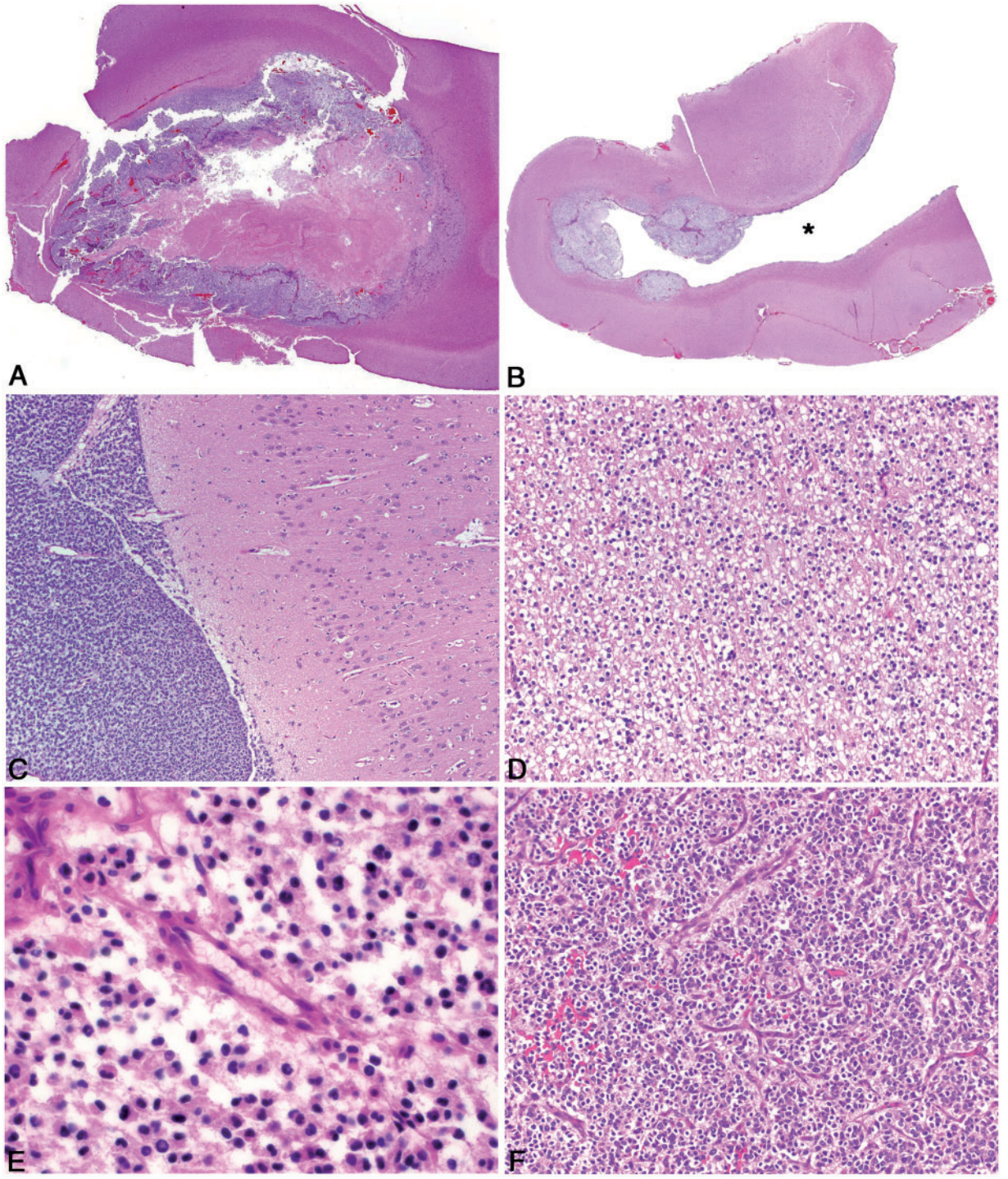

FIGURE 3. Pathologic features of canine oligodendroglioma. **(A)** High-grade oligodendroglioma in the cerebrum with effacement of the grey matter and minimal invasion of the subjacent white matter, despite the presence of multiple hallmarks of high-grade such as necrosis and microvascular proliferation. **(B)** High-grade oligodendroglioma with extensive intraventricular spread (Asterisk = ventricular lumen). **(C)** High-grade oligodendroglioma with extensive subpial and meningeal spread. **(D)** Well-differentiated oligodendrogliomas have moderate to dense cellularity, and often have processing-induced retraction of cytoplasm resulting in a "honeycomb" or "fried egg" appearance. **(E)** Features of poor fixation in canine oligodendroglioma include pyknotic nuclei, poor nuclear detail, tissue discohesion, tinctorial abnormalities, and poor stain uptake in intravascular erythrocytes. **(F)** Vascular proliferation that comprises increased numbers of congested, branching, and occasionally tortuous vessels lined by a single layer of hypertrophied endothelium, does not meet the criteria for true microvascular proliferation.

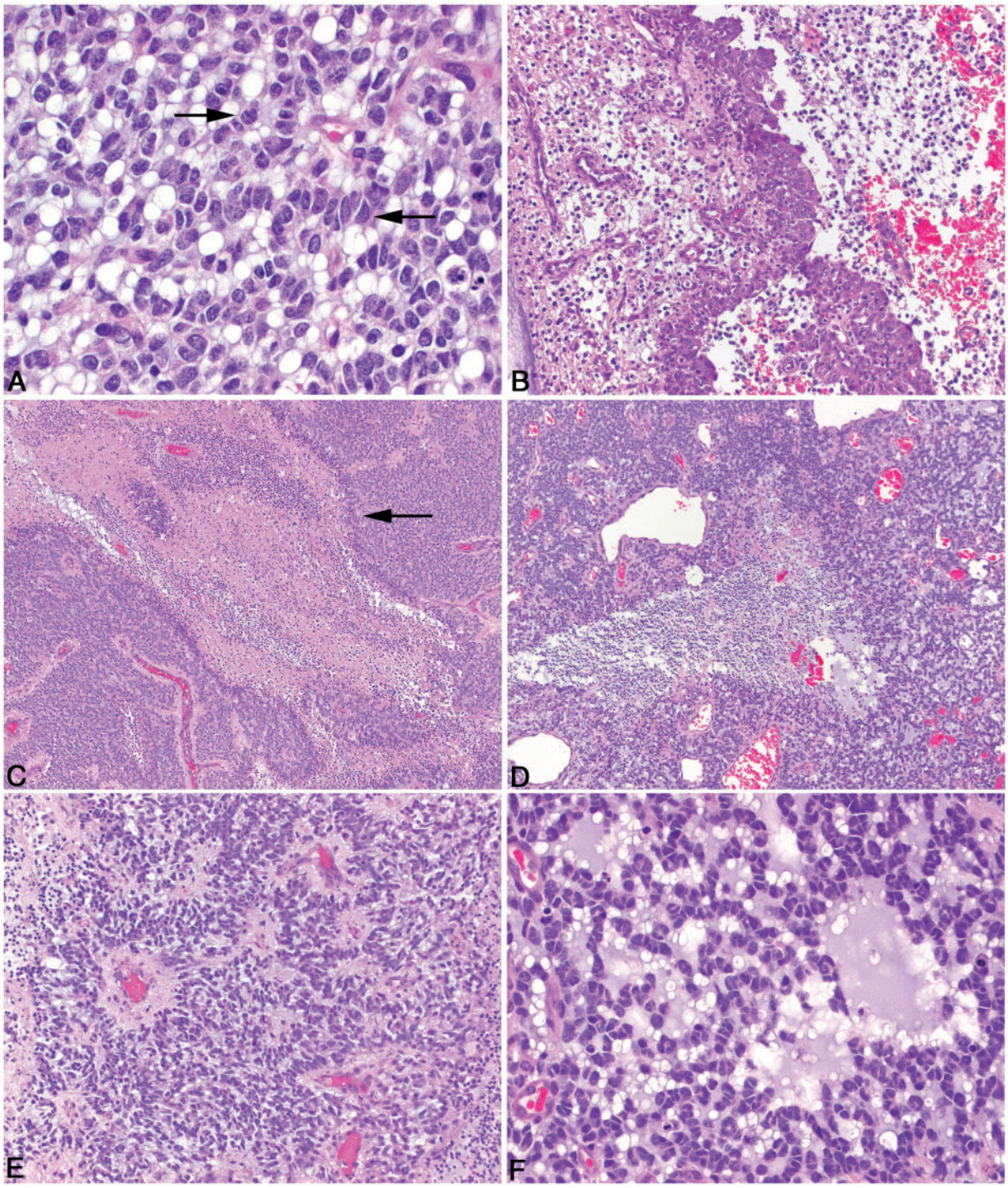

FIGURE 4. Pathologic features of canine oligodendroglioma. **(A)** In high-grade oligodendroglioma, cells with large, deeply cleaved, folded, or irregular nuclei (arrows) with occasionally pronounced nuclear molding are present. **(B)** High-grade oligodendrogliomas contain variably robust peripheral foci of microvascular proliferation characterized by tortuous clusters of vessels lined by multiple layers of endothelial cells and pericytes. **(C)** High-grade oligodendrogliomas have areas of necrosis which in some cases have cellular palisading (arrow) along the margin of the necrotic area. **(D)** In high-grade oligodendrogliomas, not all regions of necrosis are rimmed by palisading neoplastic cells. **(E)** In some oligodendrogliomas that have otherwise typical morphology, neoplastic cells are arranged in a pattern that mimics that of ependymal pseudorosettes. **(F)** Oligodendrogliomas frequently contain moderate to abundant amounts of basophilic, myxoid matrix.

demarcated, often markedly infiltrating the surrounding parenchyma (Fig. 5A). The nuclei were variable, but predominately ovoid to elongate, and they ranged from small and hyperchromatic to larger with finely stippled chromatin patterns and 1–2 small nucleoli (Fig. 5B). Visible cytoplasm was generally absent, but some tumors had cells with a small amount of eosinophilic cytoplasm. Binucleated cells were occasionally seen. Uncommon features included microcysts (Fig. 5C), foci of mineralization, and mucin deposits in the stroma. In general, low-grade astrocytomas lacked necrosis, microvascular proliferation, and easily identifiable mitotic activity. Four low-grade tumors were composed primarily of round to ovoid cells with abundant eosinophilic cytoplasm and eccentric nuclei, consistent with gemistocytic differentiation (Fig. 5D). Three gemistocytic tumors were located in the cerebellum and were more well-demarcated than other low-grade tumors. This morphology was also noted within 1 low-grade astrocytoma located within the frontal lobe.

High-grade astrocytomas varied in their growth pattern, with equal numbers showing infiltrative or expansile growth (Fig. 5E), and they were more densely cellular and exhibited more nuclear pleomorphism than low-grade tumors. Cells often had visible cytoplasm and ranged from ovoid to polygonal to spindle-shaped, and mitotic activity was readily identified (Fig. 5F). In some tumors, spindle-shaped cells predominated and were arranged in a fascicular pattern (Fig. 5F). Large areas of necrosis were often present, sometimes in a serpiginous pattern (Fig. 5E) and neoplastic cells palisaded around necrotic areas in some tumors. Microvascular proliferation was frequent. Vascular tufts were often arranged in rows, and in most tumors, were located centrally rather than peripherally. Hemorrhage and lymphocytic perivascular cuffing were common features. Less frequent findings included mineralization of necrotic areas, leptomeningeal infiltration, thrombosis, and the presence of small regions that more closely resemble oligodendroglioma. Similar to oligodendroglioma, the presence of microvascular proliferation and necrosis were the most reliable features to differentiate a low-grade astrocytoma from a high-grade astrocytoma.

Undefined Glioma

Undefined glioma was characterized as a glioma that had no predominant morphologic features that would allow it to be classified as either an oligodendroglioma or an astrocytoma. These neoplasms consisted of variable proportions of cells showing oligodendroglial and astrocytic differentiation that were geographically distinct or merging into each other (Fig. 6A, B). Importantly, if the proportion of the neoplasm was >80% oligodendroglial or astrocytic, then it was assigned to 1 of those 2 diagnoses.

Typical oligodendroglial morphologic features included closely or loosely arranged sheets of neoplastic cells supported by a fine fibrovascular stroma often containing sparse, faintly basophilic mucinous material that occasionally coalesced to form microcysts within the neoplasm (Fig. 6C). Neoplastic cells had a scant to moderate amount of eosinophilic cytoplasm often containing the typical artifactual perinuclear clear halo, and oval nuclei with dense or coarse chromatin.

Typical astrocytic features included sheets or streams of neoplastic cells supported by a fibrillary, neuropil-like stroma. These areas were typically less densely cellular than the areas with oligodendroglial differentiation. Neoplastic cells had abundant, polygonal or elongate, eosinophilic cytoplasm with indistinct cell margins and oval to elongate nuclei with finely stippled chromatin and 1–2 nucleoli. Other features shared by oligodendrogliomas and astrocytomas were also present in undefined gliomas, including areas of necrosis with or without marginal pseudopalisading of neoplastic cells, areas where neoplastic cells were palisading around capillaries in a configuration consistent with pseudo-rosettes, microvascular proliferation, and mineralization. Similar to oligodendrogliomas and astrocytomas, low- versus high-grade determination was based on the presence of necrosis (with or without pseudopalisading) and microvascular proliferation. Figure 7 depicts the typical gross appearances of canine oligodendroglioma and astrocytoma.

Immunohistochemistry

Immunohistochemistry was performed on all patients of the first cohort of reviewed cases (n = 147; 126 necropsy and 21 biopsy cases) and divided into necropsy versus biopsy for data interpretation. Consortium pathologists reviewed the IHC stains, and each case was scored using the scale noted above. Olig2 immunoreactivity was predominately nuclear with occasional less intense staining in the cytoplasm of neoplastic cells. Neoplasms for which oligodendroglioma was the majority opinion diagnosis, immunoreactivity was robust and diffuse in the neoplastic population as opposed to astrocytic tumors where the number and intensity of immunoreactive cells were decreased. For Olig2, mean immunoreactivity scores were 2.4/3 on necropsy cases and 2.7/3 on biopsy cases (Fig. 6D). GFAP immunoreactivity was diffusely cytoplasmic in the neoplastic cells and restricted to those neoplasms for which astrocytoma or undefined glioma was the majority opinion diagnosis. For GFAP, mean immunoreactivity scores were 0.6/3 on necropsy cases and 0.9/3 on biopsy cases (Fig. 6E). CNPase immunoreactivity was diffusely cytoplasmic and of variable intensity. Intensity was strongest in the biopsy cases for which oligodendroglioma was the majority opinion diagnosis. For CNPase, mean immunoreactivity scores were 0.9/3 on necropsy cases and 2.1/3 on biopsy cases (Fig. 6F). Ki67 immunoreactivity was restricted to nuclear expression in a variable number of neoplastic cells throughout the majority of cases. Mean Ki67 immunoreactivity was 0.06/3 on necropsy cases and 0.09/3 on biopsy cases. The Ki67 values were small due to large number of cases that had no immunoreactivity, even in cases where the histologic assessment (identification of mitotic figures) predicted robust Ki67 immunoreactivity. For Olig2, GFAP, CNPase, and Ki67, altered immunoreactivity of the marker due to inherent tissue abnormalities (ie tissue fixation delay, uneven fixation) was common, especially in the necropsy cases. Lastly, although neurofilament was applied to the initial cohort of cases and clearly defined the degree of tissue infiltration of the neoplasm, after review of the stains it was clear that this method did not enhance detection of infiltration to warrant its use in this series.

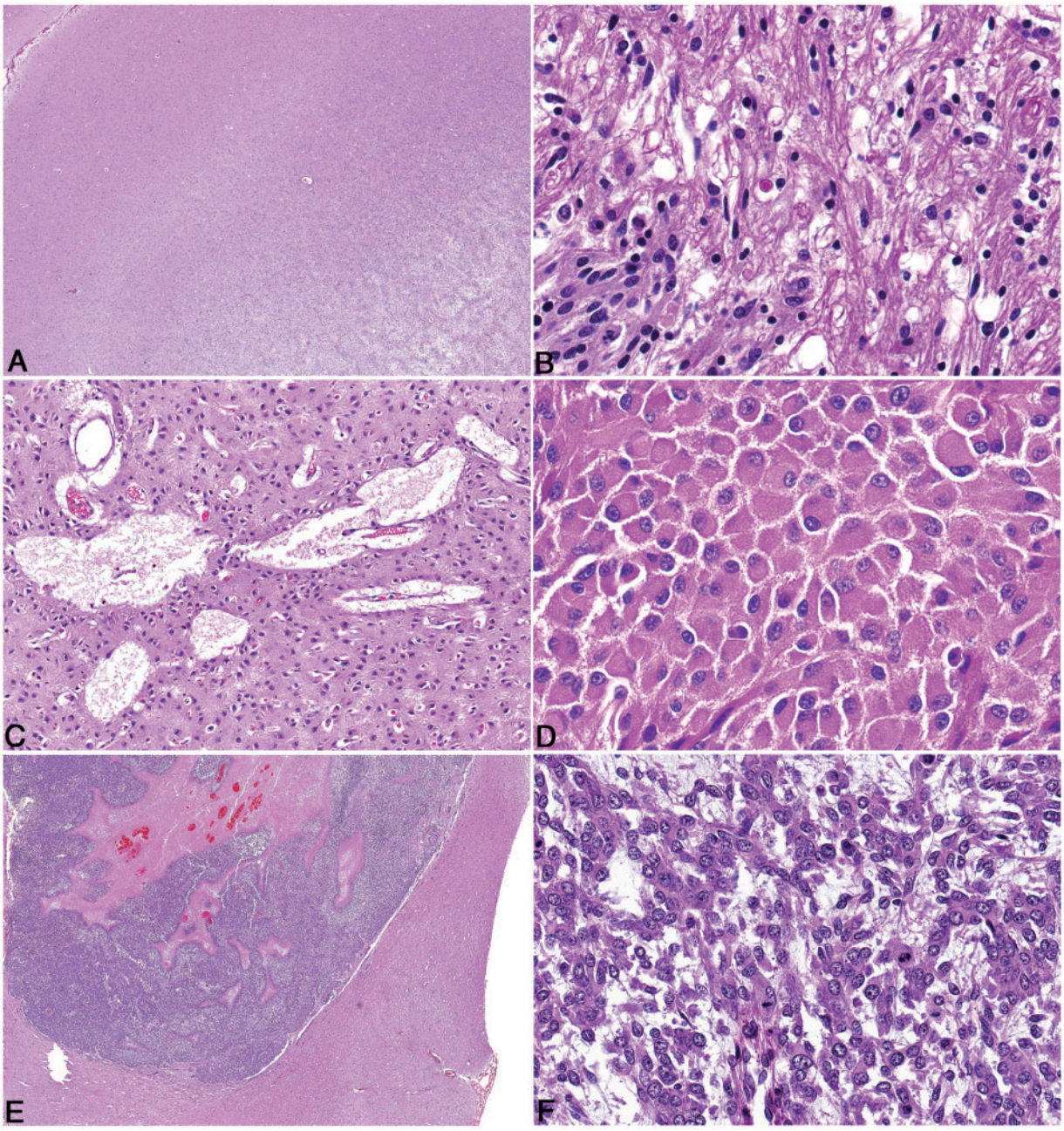

FIGURE 5. Pathologic features of canine astrocytoma. **(A)** Low-grade astrocytomas are typically invasive, variably cellular, and distorted the parenchyma. **(B)** The nuclei of neoplastic astrocytes are typically ovoid to elongate and had a wide range in size with a finely stippled chromatin pattern and 1–2 small nucleoli. **(C)** Multifocal, but scattered microcysts containing degenerate, proteinaceous material or mucin are present in some astrocytomas. **(D)** Gemistocyte-like cell morphology in a low-grade gemistocytic astrocytoma. **(E)** High-grade astrocytomas have large regions of geographic necrosis, with or without palisading along the areas of necrosis. **(F)** In some astrocytomas, interlacing fascicles of spindle cells predominate in the neoplasm.

Statistical Analysis of Reviewer Performance: Agreement and Prevalence of Histologic Features

Agreement on tumor type and tumor grade was moderate for all reviewers as well as for reviewers with the same scientific background. Reviewers had substantial agreement on the diagnosis of necrosis and microvascular proliferation (Supplementary Data Figs. S1 and S2). We found that the prevalence determined by physicians was significantly lower than that determined by veterinarians with regard to the diagnosis of oligodendroglioma, infiltration, and necrosis ($p < 0.001$), whereas it was significantly higher with respect to the diagnosis of astrocytoma and high tumor grade, as well as detection of necrosis with pseudo-palisading and microvascular proliferation ($p < 0.001$) (Supplementary Data Fig. S3).

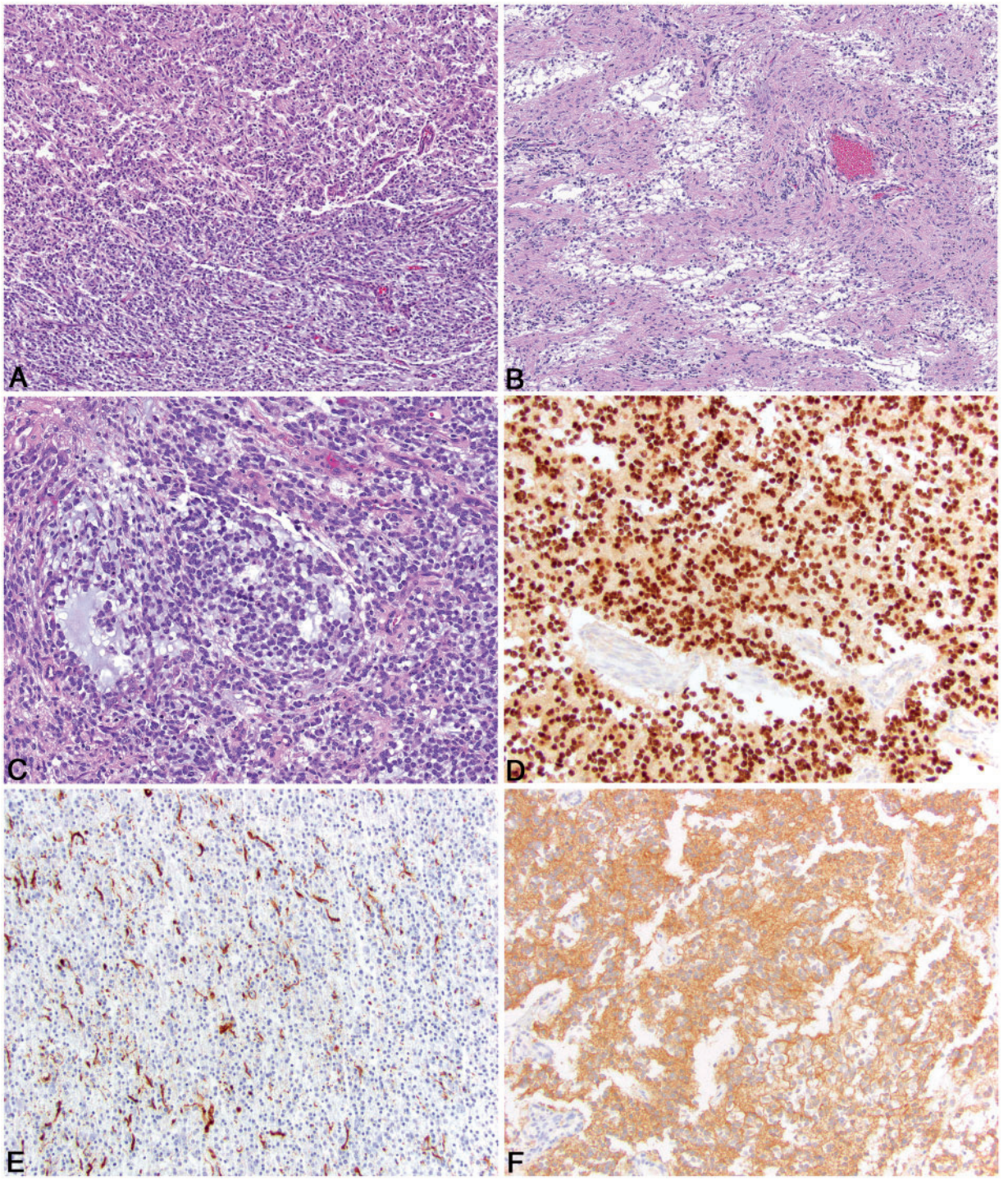

FIGURE 6. Pathologic features of undefined canine glioma and immunohistochemical features. **(A)** A roughly equal proportion of oligodendroglioma-like morphology (top) and astrocytoma-like morphology bottom). **(B)** Two distinct populations of neoplastic cells with small, basophilic cells admixed with mucin separated by islands of less dense neoplastic cells that are more astrocytic in morphology. **(C)** Regions of basophilic mucin deposition in an undefined canine glioma. **(D)** Olig2 immunoreactivity in canine oligodendroglioma is characterized by diffuse, intense intranuclear immunoreactivity in virtually all of the neoplastic cells. **(E)** GFAP immunoreactivity in canine astrocytoma is often patchy, but intense cytoplasmic immunoreactivity is noted in approximately 30% of the neoplastic cells. **(F)** CNPase immunoreactivity in canine oligodendroglioma is diffusely cytoplasmic and specific for the neoplastic cells.

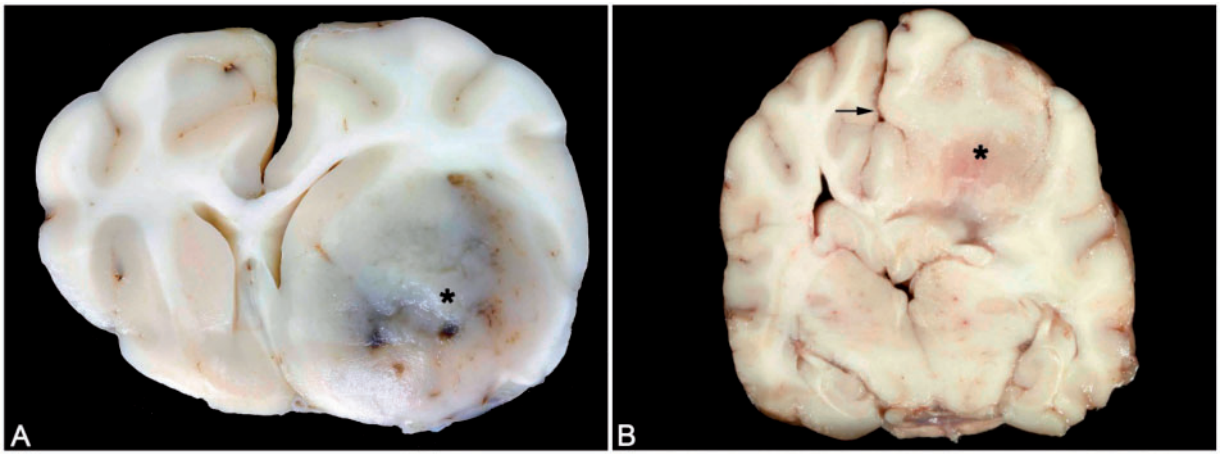

FIGURE 7. Typical gross appearances of canine oligodendroglioma and astrocytoma. **(A)** Canine oligodendroglioma. A well-demarcated, gelatinous gray mass is present in the region of the ventral frontal cortex and basal ganglia (asterisk) associated with areas of hemorrhage and a midline shift. **(B)** Canine astrocytoma. A poorly recognizable mass (asterisk) that is of similar color and consistency with the adjacent parenchyma and is associated with a midline shift (arrow).

Compared to low tumor grade, high tumor grade was associated with higher prevalence of an oligodendroglioma diagnosis, focal infiltration, necrosis, pseudo-palisading, microvascular proliferation, and mitoses (Supplementary Data Fig. S4). Gliomas in the Boston terrier, Bulldog, and Boxer breeds were associated with higher prevalence of oligodendroglioma ($p < 0.001$) and infiltration ($p = 0.011$) than other breeds. They also trended toward a higher prevalence of mitoses ($p = 0.081$) (Supplementary Data Fig. S5).

DISCUSSION

The existing classification system for canine gliomas was published in 1999 (31). Twenty years later, there has been little progress in refining this basic histologic classification. Our simplified system is an admission that there is much to learn about the histogenesis and behavior of these tumors. A more detailed system will depend on future molecular studies and more thorough clinical annotation. Some morphologic features described herein were not discussed in the 1999 publication, and we hope that a more complete histologic atlas will better inform collection of molecular data in the future.

The cases reviewed in the classification phase emphasize the importance of sample size and quality. Due to the heterogeneous nature of gliomas, it is important to recognize that biopsies, especially small samples, may not accurately reflect the overall histologic geography of the glioma sampled, and therefore may hamper consistent classification. It is particularly important to emphasize the difficulty in assessing tumor infiltration with biopsy samples; this feature should not be commented on unless normal brain parenchyma is submitted with the mass. Similarly, fixation time delays and prolonged fixation can also lead to altered histologic findings (e.g., fried-egg appearance of oligodendroglioma). Biopsy samples should be placed in 10% neutral buffered formalin promptly and shipped expediently so that the tissues can be paraffin embedded as soon as possible after tissue collection, preferably <5 days. Necropsies should be performed as soon as possible (ideally <6 hours postmortem); however, since this is often not possible in veterinary medicine, animals should be cooled quickly so that the inherent retention of body heat in a deceased dog does not accelerate autolysis.

The data presented here reinforces those of other investigators who have described the histologic landscape of canine glioma based on descriptive histopathologic diagnosis (14, 17–19, 25, 27). Dogs develop relatively more oligodendroglioma than astrocytoma based on data in Table 2, a finding supported by prior literature in this area (15–17). This is the largest canine glioma dataset to date in which standardized immunohistochemistry was used. Advanced molecular tools have largely replaced immunohistochemistry in human glioma diagnostics, but given the limited availability of genetic biomarkers in dogs, immunohistochemistry is still an important diagnostic tool for canine glioma (24, 25, 27, 38, 39). The addition of specific additional and/or different IHC markers, as supported by the forthcoming comprehensive molecular characterization initiative, may be helpful in further bridging the canine and human neuropathology worlds. It remains to be determined whether molecular classification will define additional subtypes and/or alter the diagnosis in any way, and whether this method of classification will be linked to differences in clinical outcomes within the landscape of therapeutic options for canine patients.

Olig2 appears to be more resistant to fixation-induced antigen crosslinking and is a fairly reliable marker of glial differentiation in either necropsy or biopsy cases (39). While Olig2 may not reliably differentiate between astrocytic and oligodendrocytic lineage, many of the oligodendrogliomas examined had strong, diffuse immunoreactivity, while immunoreactivity was more variable in astrocytomas. Lack of Olig2 immunoreactivity should alert the diagnostician to other potential diagnoses, including round cell neoplasms. In addition to the value of Olig2, our findings also suggest that CNPase may be a very useful marker of oliodendroglial differentiation (for biopsies in particular) if fixation time is limited. CNPase

is a myelinating enzyme specific to oligodendrocytes and Schwann cells. In the current study, CNPase immunoreactivity was low in necropsy cases; however, it was often strongly positive in biopsy cases that had features consistent with oligodendroglioma. In general, CNPase, GFAP, and Ki67 all need to be interpreted cautiously due to fixation-related alterations in immunolabeling, and 1 should consider a negative stain, especially in necropsy specimens, as an indication for additional stains and further molecular assessment as available. Traditionally, GFAP has been the gold standard immunohistochemical marker for canine astrocytic neoplasms; however, we found in the current study that its immunoreactivity was often limited, even in cases of clear astrocytic morphology. Most biopsy cases and those necropsy cases for which tissues were collected and fixed expediently had very good Ki67 immunoreactivity. However, most necropsy specimens had some degree of loss of immunoreactivity for Ki-67 that ranged from mild to complete loss, reinforcing the need to adhere to necropsy best practices if this marker is to be used. We believe that negative immunohistochemical results must be interpreted cautiously, as GFAP, CNPase, and Ki67 can all be negatively impacted by fixation (time to fixation, time in fixative, buffering of fixative).

Due to the limited availability of brain biopsy and the utilization of humane euthanasia in veterinary medicine in those circumstances when therapy is not pursued, necropsy samples of canine glioma are more readily procured than biopsy samples. This makes developing a grading scheme that can be used in prospective studies of canine glioma more difficult, as many of these patients are not clinically studied for a long period of time. Regardless, the authors have chosen to develop a simplified grading scheme in which the features of high-grade glioma were defined as the presence of large tracts of necrosis, microvascular proliferation, and an observable mitotic rate. It is important to recognize that not all features are present in a high-grade canine glioma, but rather the presence of at least 1 of these key features helps define the high-grade tumors. Future work in this area should include correlation of grade with preexisting clinical signs (e.g. severity and duration of neurologic signs), geographic location of the lesion within the brain, signalment (age, breed of dog, gender), and/or lesion size at diagnosis. As clinical management of dogs with brain tumors becomes both more sophisticated and widely available, such as through increased access to funded clinical trials, we anticipate increasing access to biopsy specimens from which correlations between tumor grade and clinical outcome data can be derived.

The statistical assessment of reviewer agreement provided interesting insights into both veterinary pathologists' and physician neuropathologists' approach to histopathologic description and diagnoses, and also highlights the landscape of the tumors that comprise both groups of pathologists' caseloads. The finding that agreement on tumor type and tumor grade was moderate for all reviewers as well as for reviewers with the same scientific background, but was substantial on the diagnosis of necrosis and microvascular proliferation, may be in part explained by the relative ease of detection of these features, in contrast to the way pathologists ultimately assimilate multiple features into a final diagnosis. This supports the assignment of necrosis and microvascular proliferation as key features that, when detected, factor more heavily into assignment of high tumor grade than other features with lower statistical agreement. Necrosis and microvascular proliferation may be straightforward features to characterize, but the subjectivity that occurs with assimilation of features into a determination of tumor type and grade may have resulted in lower overall agreement, particularly with a pathology board of this size. Overall, the agreement could have been improved with repeated case review and group discussion of the material. It is also possible that variability in the physical size of samples reviewed by this board (e.g. biopsy tissues vs tumors collected at necropsy) played a role in the detection of specific features. Creation of a freely availably annotated image library may help veterinary pathologists gain experience and a comfort level with adoption of this proposed classification scheme, which will in turn support the eventual layering-on of molecular data to identify correlative subtypes of canine tumors for their human counterparts.

Physician neuropathologists had a lower prevalence of diagnosis of oligodendroglioma, infiltration, and necrosis, compared to veterinarians ($p < 0.001$), whereas this prevalence was significantly higher with respect to the diagnosis of astrocytoma and high tumor grade, as well as detection of necrosis with pseudo-palisading and microvascular proliferation ($p < 0.001$). These findings may be a reflection of the different caseloads of physician and veterinarian neuropathologists, as well as differences in the professional training and experiences of the reviewers. Certain features, such as necrosis, robust microvascular proliferation and infiltration, appear to be more conspicuous in canine tumors than they are in human tumors. Likewise, astrocytomas appear to be much more common in humans than in dogs, based upon this collection. However, it is worth noting that the statistical analysis suggests that reviewer agreement on a diagnosis of astrocytoma, as well as the other types described, was only moderate to fair. Again, this is likely a reflection of the reviewer background and reliance on molecular data to make an astrocytoma diagnosis in human patients for the physician reviewers.

Table 2 demonstrates how the physician diagnoses compared to those compiled by the entire composite neuropathologist board, as determined by simple majority utilizing the algorithm in Figure 2, but also by physician reviewers applying the 2007 WHO guidelines for classification of human glioma. As seen in the statistical analysis, it seems likely that veterinarians were much more comfortable in assigning an oligodendroglioma diagnosis of any grade, but the proportion of tumors receiving an astrocytoma diagnosis was fairly similar between the 2 groups of pathologists. Physicians were more likely to lack agreement with histopathological data alone, which is likely a reflection of their access to molecular data as an aid in assigning a final diagnosis. In a single session of review across all 193 cases from 5 physician reviewers, we were able to arrive at a majority opinion, but not a true consensus diagnosis, for 72.6% of the tumors. Consensus among a small number of physician neuropathologist reviewers has been documented in previous work, where there was significant improvement in diagnostic concordance with repeated (up to 4) sessions of case review across 4 independent sets of gliomas

($p < 0.02$) (40, 41). Although arriving at a fully concordant diagnosis across all participating pathologists was not a goal of this effort, we demonstrated that even a single session of review can provide a reasonable concordance diagnosis among a diverse group of reviewers with this proposed simplified classification scheme.

Breed associations with certain features (infiltration, high-grade, increased mitotic activity) may point to specific molecular subtypes that may support further discovery/molecular pathogenesis studies within these breeds (42). A recent description of the genomic origins of dog breeds organized into clades demonstrated that the Boxer and Bulldog cluster together, with the Boston Terrier and French Bulldog in close proximity within a cladogram of 161 dog breeds (43). This may lend further support toward a genomic basis in tumor susceptibility, as well as a tendency to develop tumors with specific features, but further study of breed-specific molecular features is clearly needed to expand upon these observations. The 2010–2014 statistical report from Central Brain Tumor Registry of the United States (CBTRUS) provides a framework from which to interpret the demographical data of our canine glioma case set. There was a male sex predilection in our cohort of canine tumors, with an incidence rate ratio of 1.53 for all males/females, and 4.14 for sexually intact males/females. This mirrors the situation in humans, in which the incidence ratio in males ranges from 1.31 to 1.58 for all gliomas (44). The finding of male predilection in our study population is an important finding, as most North American pet dogs have been gonadectomized; this data suggests that even in the face of gonad removal there exists a sex predilection similar to humans. Likewise, the location of tumors in this study population showed a predilection for the frontal, temporal, and parietal lobes (48.6% together), which is similar to the situation in humans, in which tumors in these locations account for 57.8% of all gliomas (44). In dogs, the piriform lobe is overrepresented as well, particularly for both high- and low-grade oligodendrogliomas, although comparison with humans is difficult as this anatomic region is not specified in the CBTRUS data set. The sex and location predilections identified in this study reinforce 2 of the key similarities between canine and human tumors.

From a comparative standpoint, several features of canine glioma are worthy of further consideration as scientific opportunities for future research and discovery. From the standpoint of the physician neuropathologists, it was felt that diffuse infiltration, for which determination of gray or white matter involvement is easiest from the lowest magnification, was less common in dogs, particularly within the oligodendrogliomas. Interestingly, in many of these cases, the white matter of dogs was not involved in the neoplasm and often seemed to act as a barrier for glioma growth, whereas the gray matter was commonly infiltrated by neoplastic cells. The significance of this is not clear; however, this reflects a profound difference with respect to human glioma and may represent some inherent feature of canine white matter that inhibits invasion, or represent a distinct tumor characteristic that influences cellular interactions with white matter. Also, the large tracts of necrosis and arcades of microvascular proliferation that define high-grade glioma are best assessed at low magnification. Cellular morphology, including nuclear appearance, should be assessed at high magnification. Since these are inherently heterogeneous neoplasms, it is important to explore as much neoplastic tissue as possible to determine the prevailing morphologic patterns. This will help guide the determination of an oligodendroglial versus astrocytic neoplasm and also provide better correlation to immunohistochemical and molecular analyses.

Morphologically evaluating gliomas with a dimorphic cell population is challenging (31, 45). Most molecular studies in dogs have been based on a small number of cases and have produced variable, but not always corollary, results (20–28). Molecular genotyping data across a larger number of neoplasms may be able to pinpoint key pathways that are similar to those described for human gliomas, ultimately allowing for the reclassification of these undefined tumors into an appropriate category based on their genetic profile (23, 46–49). Comprehensive molecular characterization will also allow the development and implementation of a focused panel of biomarkers that can be readily applied to clinical veterinary pathology practice, as has been accomplished in human glioma.

This initiative sought to define, through study of a large number of cases by a collaborative board of veterinarian and physician neuropathologists, how to improve upon the current methods to classify and describe canine glioma, with the long-term goal of facilitating inclusion of molecular biomarkers into the diagnostic acumen, and improving the translatability of the dog as a preclinical model for humans. This was the first joint effort of its kind pertaining specifically to canine CNS neoplasia and could serve as a template for future comparative efforts geared toward defining the translational relevance of other canine cancers. We contend that for ongoing comparative brain tumor research, physician neuropathologist input is a key to enhancing translational value and to provide a basis for a rational approach to molecular phenotyping of both CNS and non-CNS canine tumors.

ACKNOWLEDGMENTS

The authors thank Joseph Meyer and Jen Patterson for assistance with figures and photomicrographs, respectively. The authors also thank John H Rossmeisl, Sarah Moore, Amy Durham, Rebecca Packer, Amy Hodshon, Jonathan Levine, Elizabeth Boudreau, G. Elizabeth Pluhar, Peter Dickinson, Jonathan Wood, and R. Timothy Bentley for assistance with submission of case material, and thank Cynthia Hutchinson and Lisa Parsons to Shelley Hoover for assistance with staining, slide scanning, and image management. The UNC Translational Pathology Laboratory is supported by the NCI (P30CA016086) and University Cancer Research Fund (UCRF).

REFERENCES

1. LeBlanc AK, Breen M, Choyke P, et al. Filling in the gaps for man's best friend: Perspectives from a National Academies Institute of Medicine Workshop on Comparative Oncology. Sci Transl Med 2016;8: 324ps5
2. Paoloni M, Khanna C. Translation of new cancer treatments from pet dogs to humans. Nat Rev Cancer 2008;8:147–56
3. Rowell JL, McCarthy DO, Alvarez CE. Dog models of naturally occurring cancer. Trends Mol Med 2011;17:380–8
4. Khanna C, London C, Vail D, et al. Guiding the optimal translation of new cancer treatments from canine to human cancer patients. Clin Cancer Res 2009;15:5671–7

5. Vail DM, MacEwen EG. Spontaneously occurring tumors of companion animals as models for human cancer. Cancer Invest 2000;18:781–92
6. LeBlanc AK, Mazcko C, Brown DE, et al. Creation of an NCI comparative brain tumor consortium: Informing the translation of new knowledge from canine to human brain tumor patients. Neuro Oncol 2016;18: 1209–18
7. Dhawan D, Paoloni M, Shukradas S, et al. Comparative gene expression analyses identify luminal and basal subtypes of canine invasive urothelial carcinoma that mimic patterns in human invasive bladder cancer. PLoS One 2015;10:e0136688
8. Paoloni M, Davis S, Lana S, et al. Canine tumor cross-species genomics uncovers targets linked to osteosarcoma progression. BMC Genomics 2009;10:625
9. Simpson RM, Bastian BC, Michael HT, et al. Sporadic naturally occurring melanoma in dogs as a preclinical model for human melanoma. Pigment Cell Melanoma Res 2014;27:37–47
10. Nguyen F, Peña L, Ibisch C, et al. Canine invasive mammary carcinomas as models of human breast cancer. Part 1: Natural history and prognostic factors. Breast Cancer Res Treat 2018;167:635–48
11. Al-Khan AA, Gunn HJ, Day MJ, et al. Immunohistochemical validation of spontaneously arising canine osteosarcoma as a model for human osteosarcoma. J Comp Pathol 2017;157:256–65
12. Lenting K, Verhaak R, ter Laan M, et al. Glioma: Experimental models and reality. Acta Neuropathol 2017;133:263–82
13. McNeill R, Stuhlmiller T, Bash R, et al. TMOD-01. Functional kinome characterization of a diverse panel of glioblastoma models. Neuro Oncol 2016;18:vi206–7
14. Candolfi M, Curtin JF, Nichols WS, et al. Intracranial glioblastoma models in preclinical neuro-oncology: Neuropathological characterization and tumor progression. J Neurooncol 2007;85:133–48
15. Dickinson PJ. Advances in diagnostic and treatment modalities for intracranial tumors. J Vet Intern Med 2014;28:1165–85
16. Bentley RT, Ahmed AU, Yanke AB, et al. Dogs are man's best friend: In sickness and in health. Neuro Oncol 2017;19:312–22
17. Song RB, Vite CH, Bradley CW, et al. Postmortem evaluation of 435 cases of intracranial neoplasia in dogs and relationship of neoplasm with breed, age, and body weight. J Vet Intern Med 2013;27:1143–52
18. Snyder JM, Shofer FS, Van Winkle TJ, et al. Canine intracranial primary neoplasia: 173 cases (1986-2003). J Vet Intern Med 2006;20:669–75
19. Lipsitz D, Higgins RJ, Kortz GD, et al. Glioblastoma multiforme: Clinical findings, magnetic resonance imaging, and pathology in five dogs. Vet Pathol 2003;40:659–69
20. Reitman ZJ, Olby NJ, Mariani CL, et al. IDH1 and IDH2 hotspot mutations are not found in canine glioma. Int J Cancer 2010;127:245–6
21. York D, Higgins RJ, LeCouteur TA, et al. TP53 mutations in canine brain tumors. Vet Pathol 2012;49:796–801
22. Connolly NP, Shetty AC, Stokum JA, et al. Cross-species transcriptional analysis reveals conserved and host-specific neoplastic processes in mammalian glioma. Sci Rep 2018;8:1180
23. Dickinson PJ, York D, Higgins RJ, et al. Chromosomal aberrations in canine gliomas define candidate genes and common pathways in dogs and humans. J Neuropathol Exp Neurol 2016;75:700–10
24. Fraser AR, Bacci B, le Chevoir MA, et al. Epidermal growth factor receptor and Ki-67 expression in canine gliomas. Vet Pathol 2016;53: 1131–7
25. Higgins RJ, Dickinson PJ, LeCouteur RA, et al. Spontaneous canine gliomas: Overexpression of EGFR, PDGFRalpha and IGFBP2 demonstrated by tissue microarray immunophenotyping. J Neurooncol 2010;98:49–55
26. Thomas R, Duke SE, Wang HJ, et al. 'Putting our heads together': Insights into genomic conservation between human and canine intracranial tumors. J Neurooncol 2009;94:333–49
27. Stoica G, Kim HT, Hall DG, et al. Morphology, immunohistochemistry, and genetic alterations in dog astrocytomas. Vet Pathol 2004;41:10–9
28. Filley A, Henriquez M, Bhowmik T, et al. Immunologic and gene expression profiles of spontaneous canine oligodendrogliomas. J Neurooncol 2018;137:469–79
29. Pandith AA, Qasim I, Zahoor W, et al. Concordant association validates MGMT methylation and protein expression as favorable prognostic factors in glioma patients on alkylating chemotherapy (Temozolomide). Sci Rep 2018;8:6704
30. Bush NA, Butowski N. The effect of molecular diagnostics on the treatment of glioma. Curr Oncol Rep 2017;19:26
31. Koestner A, Bilzer T, Fatzer R, et al. Histological Classification of Tumors of the Nervous System of Domestic Animals. Washington, DC: Armed Forces Institute of Pathology 1999
32. Louis DN, Perry A, Reifenberger G, et al. The 2016 world health organization classification of tumors of the central nervous system: A summary. Acta Neuropathol 2016;131803–20
33. Louis DN, Ohgaki H, Wiestler OD, et al. The 2007 WHO classification of tumours of the central nervous system. Acta Neuropathol 2007;114: 97–109
34. Fleiss JL, Cohen J. The equivalence of weighted kappa and the intraclass correlation coefficient as measures of reliability. Educ Psychol Meas 1973;33:613–9
35. Landis JR, Koch GG. The measurement of observer agreement for categorical data. Biometrics 1977;33:159–74
36. Fleiss JL. Measuring nominal scale agreement among many raters. Psychol Bull 1981;76:378–82
37. Sato K, Rorke LB. Vascular bundles and wickerworks in childhood brain tumors. Pediatr Neurosci 1989;15:105–10
38. Stoica G, Levine J, Wolff J, et al. Canine astrocytic tumors: A comparative review. Vet Pathol 2011;48:266–75
39. Johnson GC, Coates JR, Wininger F. Diagnostic immunohistochemistry of canine and feline intracalvarial tumors in the age of brain biopsies. Vet Pathol 2014;51:146–60
40. Coons SW, Johnson PC, Scheithauer BW, et al. Improving diagnostic accuracy and interobserver concordance in the classification and grading of primary gliomas. Cancer 1997;79:1381–93
41. van den Bent MJ. Interobserver variation of the histopathological diagnosis in clinical trials on glioma: A clinician's perspective. Acta Neuropathol 2010;120:297–304
42. Truvé K, Dickinson P, Xiong A, et al. Utilizing the dog genome in the search for novel candidate genes involved in glioma. Development-genome wide association mapping followed by targeted massive parallel sequencing identifies a strongly associated locus. PLoS Genet 2016;12: e1006000
43. Parker HG, Dreger DL, Rimbault M, et al. Genomic analyses reveal the influence of geographic origin, migration and hybridization on modern dog breed development. Cell Rep 2017;19:697–708
44. Ostrom QT, Gittleman H, Liao P, et al. CBTRUS statistical report: Primary brain and other central nervous system tumors diagnosed in the United States in 2010–2014. Neuro Oncol 2017;19:v1–v88.
45. Vandevelde M, Higgins RJ, Oevermann A, Veterinary Neuropathology: Essentials of Theory and Practice. Ames, IA:Wiley 2012
46. Appin CL, Brat DJ. Molecular genetics of gliomas. Cancer J 2014;20: 66–72
47. Sahm F, Reuss D, Koelsche C, et al. Farewell to oligoastrocytoma: In situ molecular genetics favor classification as either oligodendroglioma or astrocytoma. Acta Neuropathol 2014;128:551–9
48. Huse JT, Diamond EL, Wang L, et al. Mixed glioma with molecular features of composite oligodendroglioma and astrocytoma: A true "oligoastrocytoma"?. Acta Neuropathol 2015;129:151–3
49. Ceccarelli M, Barthel FP, Malta TM, et al. Molecular profiling reveals biologically discrete subsets and pathways of progression in diffuse glioma. Cell 2016;164:550–63